POAC '99
Espoo, Finland

Proceedings of the 15th
International Conference on
Port and Ocean Engineering
under Arctic Conditions

CRUSHING PROCESSES DURING EDGE INDENTATION OF ICE SHEETS

Devinder S. Sodhi
U. S. Army Cold Regions Research and Engineering Laboratory
72 Lyme Road, Hanover, NH 03755-1290, USA

ABSTRACT

The results of small-scale and medium-scale indentation tests indicate that ductile and brittle modes of ice crushing depend on the rate of indentation. A ductile-to-brittle transition was found to be at an indentation speed between 0.3 and 3 mm s^{-1} for edge indentation of a sheet of sea ice, whereas a transition speed of 3.16 mm s^{-1} has been reported for spherical indentors moving into an ice wall of a multi-year ridge. Based on experimental results with compliant structures, each cycle of an intermittent crushing event is the result of ductile and brittle crushing depending on the actual indentation rate of an indentor into an ice sheet. Besides ductile-to-brittle transition speed, which is only applicable to rigid structures, there are two transition speeds when the ice interaction with a compliant structure changes from continuous ductile to intermittent crushing and from intermittent to continuous brittle crushing. A model of non-simultaneous brittle crushing has been extended to derive an expression for the aspect ratio (structure width to ice thickness) effect found during indentation tests, and to estimate the ratio of local maximum to global maximum effective pressure on structures. To relate the results of small-scale indentation tests to full-scale situations, it has been suggested that the similarity principles of replica modeling be used, in which the model is made of the same material as the prototype but scaled in size. To validate replica modeling, the approach is to compare the effective pressure measured during small-scale tests having high aspect ratio with full-scale measurements on Molikpaq for the same indentation rate. The effective pressures during indentation into an ice wall are expected to be different from those during edge indentation into an ice sheet because of different geometry and confinement.

1. INTRODUCTION

In the past three decades, many investigators have conducted small-scale and medium-scale indentation tests to understand the processes taking place during ice crushing and to develop theoretical models for these processes. The effects of indentation speed on the mode of crushing failure have been identified: creep deformation of ice at low speed, and continuous brittle crushing at high speed (Sodhi et al. 1998). Creep deformation of ice leads to simultaneous contact between an advancing ice sheet and a structure, whereas brittle crushing results from fracture and brittle flaking of ice and leads to non-simultaneous or non-uniform contact across the width of a structure. Besides these two modes of ice crushing, there are three modes of ice interactions with compliant structures, depending on the ice speed and structural stiffness: (a) creep deformation of ice at low speed with no structural vibration, (b) intermittent crushing at intermediate speeds with considerable structural vibration, and (c)

CRUSHING PROCESSES DURING EDGE INDENTATION OF ICE SHEETS

Devinder S. Sodhi
U. S. Army Cold Regions Research and Engineering Laboratory
72 Lyme Road, Hanover, NH 03755-1290, USA

ABSTRACT

The results of small-scale and medium-scale indentation tests indicate that ductile and brittle modes of ice crushing depend on the rate of indentation. A ductile-to-brittle transition was found to be at an indentation speed between 0.3 and 3 mm s^{-1} for edge indentation of a sheet of sea ice, whereas a transition speed of 3.16 mm s^{-1} has been reported for spherical indentors moving into an ice wall of a multi-year ridge. Based on experimental results with compliant structures, each cycle of an intermittent crushing event is the result of ductile and brittle crushing depending on the actual indentation rate of an indentor into an ice sheet. Besides ductile-to-brittle transition speed, which is only applicable to rigid structures, there are two transition speeds when the ice interaction with a compliant structure changes from continuous ductile to intermittent crushing and from intermittent to continuous brittle crushing. A model of non-simultaneous brittle crushing has been extended to derive an expression for the aspect ratio (structure width to ice thickness) effect found during indentation tests, and to estimate the ratio of local maximum to global maximum effective pressure on structures. To relate the results of small-scale indentation tests to full-scale situations, it has been suggested that the similarity principles of replica modeling be used, in which the model is made of the same material as the prototype but scaled in size. To validate replica modeling, the approach is to compare the effective pressure measured during small-scale tests having high aspect ratio with full-scale measurements on Molikpaq for the same indentation rate. The effective pressures during indentation into an ice wall are expected to be different from those during edge indentation into an ice sheet because of different geometry and confinement.

1. INTRODUCTION

In the past three decades, many investigators have conducted small-scale and medium-scale indentation tests to understand the processes taking place during ice crushing and to develop theoretical models for these processes. The effects of indentation speed on the mode of crushing failure have been identified: creep deformation of ice at low speed, and continuous brittle crushing at high speed (Sodhi et al. 1998). Creep deformation of ice leads to simultaneous contact between an advancing ice sheet and a structure, whereas brittle crushing results from fracture and brittle flaking of ice and leads to non-simultaneous or non-uniform contact across the width of a structure. Besides these two modes of ice crushing, there are three modes of ice interactions with compliant structures, depending on the ice speed and structural stiffness: (a) creep deformation of ice at low speed with no structural vibration, (b) intermittent crushing at intermediate speeds with considerable structural vibration, and (c)

continuous brittle crushing at high speed with small vibrations (Sodhi 1991). Thus there are two transition speeds in between the above three modes of ice interaction with a compliant structure.

In this paper, I present a formulation to deduce the aspect ratio effect observed by many investigators during indentation tests at high speeds, and discuss estimation of global load from measurements of forces with instrumented panels over a small area of a structure. To relate the effective pressure during small-scale indentation tests, I refer to the data obtained from instruments installed on the Molikpaq structure (Wright et al. 1986, Neth 1989, Wright and Timco 1994, Hardy et al. 1998). Though indentation into an ice wall deserves considerable attention, I discuss this briefly to point out that the effective pressures measured during these tests are expected to be different from those obtained from edge indentation tests because of differences in geometry and confinement.

2. INDENTATION AGAINST THE EDGES OF ICE SHEETS

Under the sponsorship of Japan Ocean Industries Association, medium-scale indentation tests have been conducted since 1996 by pushing a segmented indentor against the edges of sea ice at constant indentation speeds in a harbor located near Abashiri, Hokkaido, Japan (Sodhi et al. 1998). In 1998, we installed four tactile sensors on the face of the indentor to measure interfacial pressure during tests at three indentation speeds (0.3, 3, 30 mm s^{-1}), while measuring forces in each of the 15 segments with load cells. We obtained data on the actual contact area and the relative magnitude of interfacial pressure from the tactile sensors. The main results of these tests were that we observed a 'line-like' contact, similar to those observed by Joensuu and Riska (1989), during high-speed (3 and 30 mm s^{-1}) indentation tests, and a gradually enlarging contact area attributable to creep deformation of ice during low-speed (0.3 mm s^{-1}) indentation tests. During the high-speed tests, the interfacial pressure within the line-like contact was high and non-uniform, and persisted at one location for a short time (100–150 ms). During the low-speed tests, the interfacial pressure was uniform and low, but the contact persisted at all times and remained simultaneous across the width of the indentor, resulting in a higher force in comparison to those generated during high-speed indentation. These two modes of ice crushing are brittle flaking at high speed and ductile or creep deformation at low speed. Brittle flaking results from the rapid increase in interfacial pressure because of elastic deformation and the ensuing crack nucleation and propagation, whereas creep deformation and stress relaxation prevent the increase of interfacial pressure to a level necessary to fracture ice. With an increase in indentation speed during interaction with a rigid structure, the failure mode changes from creep deformation to brittle flaking at some transition speed, which was between 0.3 and 3 mm s^{-1} for the indentation tests in Japan. It is possible for the ductile-to-brittle transition speed to depend on ice temperature, because the ice properties are highly dependent on how close its temperature is to the melting point.

Theoretical treatment of creep indentation into the edges of ice sheets exists in the current literature, and it should be possible to determine the ice force on a structure of any size because the creep properties are independent of scale (Ponter et al. 1983). However, theoretical formulation of the brittle crushing process has begun to emerge through experimentation and measurements as non-simultaneous brittle flaking. The results of indentation tests using segmented indentors (Sodhi 1998) showed that the correlation between

forces measured in different segments decreased with an increase in indentation speed. This is attributed to the failure modes of ice having simultaneous contact across the width of an indentor at low indentation speed and non-simultaneous contact as a result of brittle crushing at high indentation speed.

In the case of a compliant structure, the force resulting from ice–structure interaction deforms the structure, and this causes variable rates of indentation into an ice sheet. This rate is the difference between the speed of a point on the ice sheet at some distance from the structure with respect to a fixed datum and the rate of the structure's deflection or displacement (Sodhi 1991, 1995). If the indentation rate into an ice sheet falls below the ductile-to-brittle-transition speed, the ice undergoes ductile deformation, resulting in the buildup of the interaction force. When the ice fails at some force level, the structure moves forward into the ice at high speed while crushing the ice ahead of it in brittle flaking. Depending on the structural stiffness and damping, the structure may separate from the ice edge while executing transient oscillations. When the kinetic energy of the structure is dissipated in brittle crushing of ice and the indentation rate is below the transition speed, this cycle starts again with the ductile deformation of ice and increase in load on the structure. A repeated sequence of these events results in intermittent crushing (Sodhi 1991). Intermittent crushing has been simulated as a series of processes alternating between ductile deformation and brittle flaking (Sodhi 1995). Experimental verification of this switching between ductile and brittle modes of crushing during one cycle of intermittent crushing is the main objective of recent ice-structure interaction tests at CRREL. During these tests, I measure the interfacial contact area and relative magnitude of ice pressure by installing with tactile sensors at the ice-structure interface. Early results show that this switching of ice crushing modes does take place. I shall report the results of these tests fully in a later publication. Thus there are two transition speeds during ice interaction with compliant structures: from continuous ductile to intermittent ductile-brittle crushing and from intermittent to continuous brittle crushing.

During measurements of full-scale ice forces on Molikpaq, severe vibrations were not experienced during ice crushing events when the ice drift speed was more than 100 mm s^{-1}. However, the ice moved in a stop–start manner and caused structural vibrations when radar measurements indicated that the ice drift speed was between 10 and 50 mm s^{-1} (Hardy et al. 1998). This experience can be explained according to the modes of ice interaction with a compliant structure. At higher speeds, the ice failed continuously in the brittle mode, causing some vibrations, whereas ice failed in the intermittent crushing mode during interactions at lower ice speeds and caused severe vibrations.

2.1 Aspect Ratio Effect

On the basis of results of small-scale indentation tests, Afanasyev et al. (1972) were the first to propose that there is a dependence of the effective pressure on the aspect ratio (defined as the ratio of structure width w to ice thickness h). Others have also found this effect from the results of their small-scale tests. For ductile deformation, the indentation factor is the ratio of effective pressure to the yield stress of the material (Hill 1950). Dependence of the indentation factor on the aspect ratio during ductile failure is similar to that during brittle failure. However, there is a need to understand the difference between these two factors. I propose that we use an indentation factor derived from a plasticity analysis to estimate the effective

pressure measured during creep deformation of ice. On the other hand, the relative pressure obtained empirically from indentation test results should be used to estimate the effective pressure during brittle crushing failure of ice. In this paper, I shall restrict my discussion to relative pressure at various aspect ratios during brittle crushing.

Line-like contact areas were observed during edge indentation of ice sheets at high speeds (Joensuu and Riska 1989, Sodhi et al. 1998). Similarly, line-like contacts were also observed during medium-scale indentation tests at Hobson's Choice Ice Island in 1990 via video recordings through a transparent window in the indentor (Frederking et al. 1990, Masterson et al. 1993, Gagnon 1998). On the basis of these latter observations, Spencer and Masterson (1993) proposed that the real contact area during edge indentation would have a line-like shape in the middle and diagonal lines near the ends of an indentor. However, the experimental results do not support this assumption. After the Rational Evaluation of Ice Forces on Structures (REIFS) Workshop held in Mombetsu, Japan, a group of international researchers visited the JOIA experimental site on 4 February 1999 and saw an indentation test with tactile sensors installed at the interface between the edge of an ice sheet and the indentor. The data from the tactile sensors showed a line-like contact in the middle of the ice sheet across the 1.5-m-wide indentor, but did not show diagonal lines near the ends. Moreover, the pressure within the line-like contact is not constant, as assumed by Spencer and Masterson (1993), but highly variable with respect to time and position.

The aspect ratio effect can be obtained from non-simultaneous failure of ice in different regions of an indentor, as proposed by Kry (1978) and Ashby et al. (1986). However, they did not consider the correlation of ice forces generated in different points of an indentor. To include the correlation of non-simultaneous forces, Dunwoody (1991) considered the global force to be given by

$$g(t) = \int_w f(x,t)dx, \tag{1}$$

where $f(x, t)$ is the local force per unit width of the structure, x is the position of a point on the structure, t is the time, and w is the width of the structure. The variation of local force across the width depends on the number of contacts and the size of crushing zones. Under the assumption that the ice failure process is uniformly same across the width of the structure, the average local force per unit width $\mu_{f(t)}$ is independent of the position of a point on the structure, implying the average global force $\mu_{g(t)} = E[g(t)] = wE[f(t)] = w\mu_{f(t)}$.

Dunwoody (1991) proposed a spatial correlation function in terms of a negative exponential function:

$$R_{f(t)}(x_2 - x_1) - (E[f(t)])^2 = \sigma^2_{f(t)} \exp(-\frac{|x|}{L}), \tag{2}$$

where $R_{f(t)}(x_2-x_1)$ is the auto-covariance function of the local force $f(t)$, x is the distance between two points at x_2 and x_1 on the structure, $\sigma_{f(t)}$ is the standard deviation of the local force $f(t)$, and L is a length parameter in the above expression to express correlation of forces over a distance and may be related to the size and density of crushing zones. Sodhi et al. (1998) shows plots of correlation coefficient versus distance, from which an estimate of correlation L can be made.

The standard deviation of the global force (Dunwoody 1991, Sodhi 1998) is given by:

$$\sigma_{g(t)}^2 = 2L\sigma_{f(t)}^2\left[w - L\left\{1-\exp\left(-\frac{w}{L}\right)\right\}\right]. \quad (3)$$

The maximum global force on the structure is given by: $F_{\max} = \mu_{g(t)} + 3\sigma_{g(t)}$, assuming normal distribution and probability of exceedance equal to 0.0013. Dividing both sides by wh, we get the maximum effective pressure:

$$p_{\max} = \frac{F_{\max}}{wh} = \frac{\mu_{g(t)}}{wh} + 3\frac{\sigma_{g(t)}}{wh} = \frac{\mu_{f(t)}}{h} + 3\frac{\sigma_{f(t)}}{h}\sqrt{2\frac{L}{w}\left[1-\frac{L}{w}\left(1-e^{-\frac{w}{L}}\right)\right]} \quad (4)$$

Dividing both sides by $\mu_{f(t)}/h$, we get the following expression for the relative pressure:

$$\frac{p_{\max}}{\mu_{f(t)}/h} = 1 + 3\frac{\sigma_{f(t)}}{\mu_{f(t)}}\sqrt{2\frac{L}{h}\frac{h}{w}\left[1-\frac{L}{h}\frac{h}{w}\left(1-e^{-\frac{w}{h}\frac{h}{L}}\right)\right]}, \quad (5)$$

where $\sigma_{f(t)}/\mu_{f(t)}$ is the coefficient of variation of the local load per unit width. Figure 1 shows plots of the relative pressure vs. aspect ratio for three values of the coefficient of variation ($\sigma_{f(t)}/\mu_{f(t)}$ = 2.0, 1.0, and 0.5) and h/L = 10.

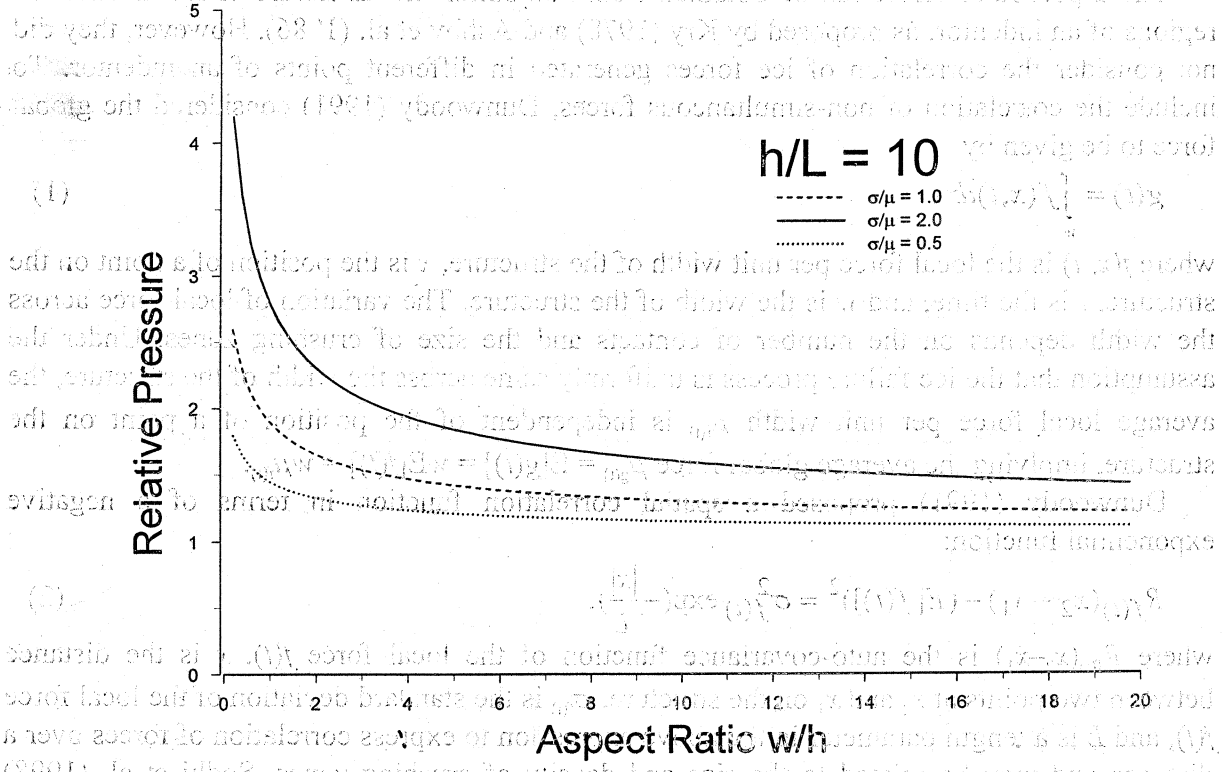

Figure 1. Plots of relative pressure $\frac{p_{\max}}{\mu_{f(t)}/h}$ vs. aspect ratio $\frac{w}{h}$.

2.2. Comparison of Small-Scale and Full-Scale Data

To relate the effective pressure measured during small-scale tests to full-scale situations, Sodhi (1992, 1998) proposed similarity principles according to replica modeling (Baker et al. 1973) for brittle crushing during edge indentation of ice sheets at high speeds. As mentioned earlier, brittle crushing took place against the Molikpaq structure when the ice drift speed was higher than 100 mm s^{-1}. Because much of the Molikpaq data is still proprietary, it is difficult to relate the published data with respect to ice drift speed. Figure 2a shows plots of ice effective pressure measured on Molikpaq vs. ice contact length for first-year ice having thickness in the range of 0.5 and 1.5 m (Wright et al. 1986). Figure 2b shows plots of ice effective pressure vs. ice thickness during crushing failure of first-year ice against the Molikpaq structure at the Tarsuit P-45 and Amauligak I-65 locations (Wright and Timco 1994). The ice pressure is high for small contact length, in comparison to that for longer contact length, and is in the range of values between 1 and 3 MPa.

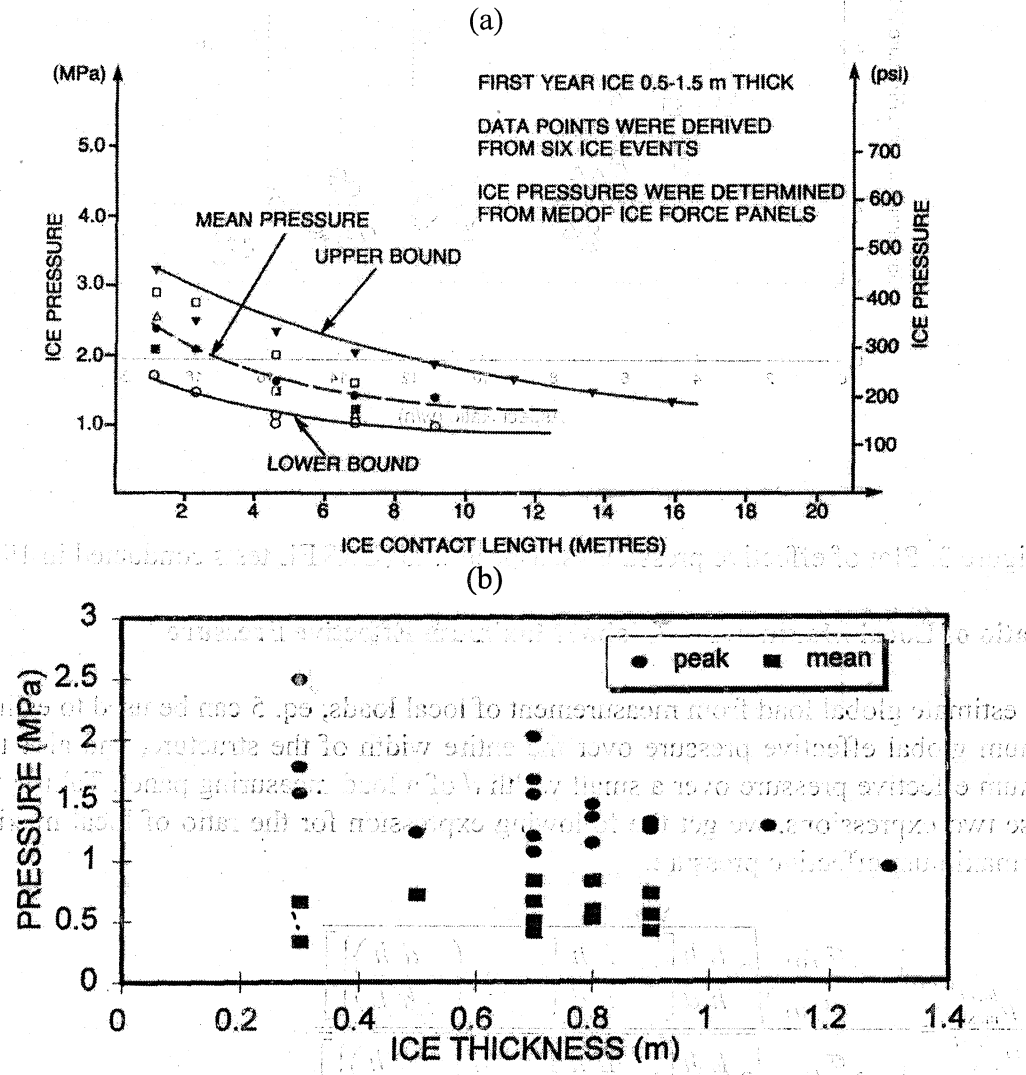

Figure 2. Molikpaq ice pressure measured at (a) Tarsuit P-45 (from Wright et al. 1986), and (b) Tarsuit P-45 and Amauligak I-65 (from Wright and Timco 1994).

Figure 3 shows plots of small-scale data on effective pressure obtained from indentation tests in freshwater ice at speeds greater than 100 mm s^{-1}. Similar to the plots in Figure 1, the effective pressure remains constant for large aspect ratios (>8). The effective pressure for large aspect ratio (>8) is in the range of 1.25 and 2.5 MPa, which is within the range of effective pressures measured during crushing failure of ice against Molikpaq. In my opinion, good agreement between these two sets of data validates the similarity principles according replica modeling.

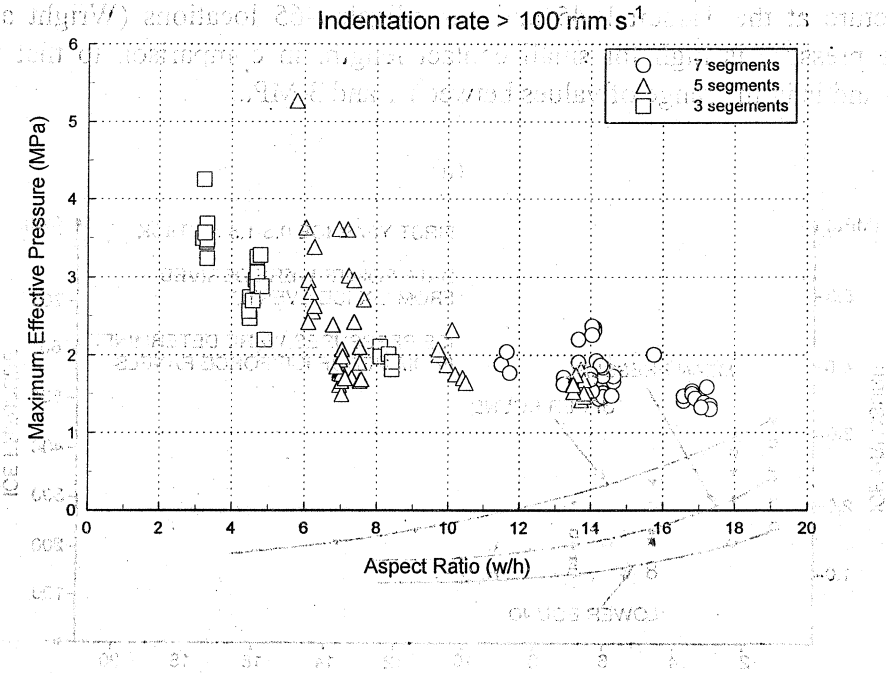

Figure 3. Plot of effective pressure vs. aspect ratio (CRREL tests conducted in 1991-92)

2.3 Ratio of Local Maximum to Global Maximum Effective Pressure

To estimate global load from measurement of local loads, eq. 5 can be used to estimate the maximum global effective pressure over the entire width of the structure, and also the local maximum effective pressure over a small width d of a load measuring panel. Taking the ratio of these two expressions, we get the following expression for the ratio of local maximum to global maximum effective pressure:

$$\frac{p_{\max}^{local}}{p_{\max}^{global}} = \frac{1+3\dfrac{\sigma_{f(l)}}{\mu_{f(l)}}\sqrt{2\dfrac{L}{h}\dfrac{h}{d}\left[1-\dfrac{L}{h}\dfrac{h}{d}\left\{1-\exp\left(-\dfrac{d}{h}\dfrac{h}{L}\right)\right\}\right]}}{1+3\dfrac{\sigma_{f(l)}}{\mu_{f(l)}}\sqrt{2\dfrac{L}{h}\dfrac{h}{w}\left[1-\dfrac{L}{h}\dfrac{h}{w}\left\{1-\exp\left(-\dfrac{w}{h}\dfrac{h}{L}\right)\right\}\right]}}. \qquad (6)$$

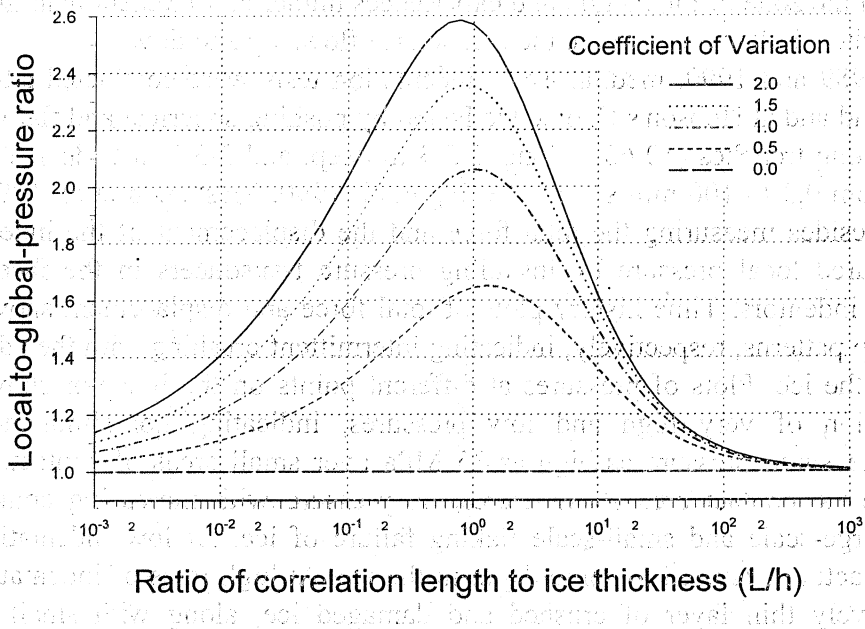

Figure 4. Plots of local-to-global ratio vs. L/h for w/h=59 and d/h=2.27.

Figure 4 shows plots of the ratio of local to global effective pressure versus L/h for w/h = 59, d/h = 2.27, and various values of the coefficient of variation $\sigma_{f(t)}/\mu_{f(t)}$ of local force per unit width. Ratios of w/h = 59 and d/h = 2.27 pertain to the dimensions of the Molikpaq structure and the Medof panels for an ice thickness of 1 m (Hardy et al. 1998). As shown in Figure 4, the pressure ratio is close to 1 for very large or very small values of L/h, and reaches a maximum for L/h close to 1. In Figure 4, the maximum value of this ratio is between 1 and 3, depending on the coefficient of variation $\sigma_{f(t)}/\mu_{f(t)}$. The reason for this ratio to be close to 1 for very large or very small values of L/h can be attributed to the mode of ice crushing associated with L/h. Very large values of L/h mean simultaneous crushing with perfect correlation of ice forces in all segments, as would be the case in ductile deformation of ice. Very small values of L/h mean non-simultaneous crushing, with no correlation of ice forces in various segments of the indentor, as would be the case in brittle flaking failure of ice. The actual case lies in-between these two extreme cases. The coefficient of variation $\sigma_{f(t)}/\mu_{f(t)}$ of local force per unit width also depends on the mode of ice crushing, because it is high in simultaneous ice failure, and low for continuous ice crushing. Wright et al. (1986) have estimated the face (global) and group (local) effective pressures (Fig. 2a), and it appears that their estimation of the ratio of local to global effective pressure is in agreement with the ratios plotted in Figure 4.

3. INDENTATION INTO ICE WALLS

In 1984, a group of oil companies conducted indentation tests in a tunnel dug into a grounded iceberg at Pond Inlet (Benoit et al. 1984). The same apparatus has been used for indentation tests conducted in trenches made in multi-year ice. The crushed ice flows out in all directions from the zone of interaction and experiences higher confinement than that found in the case of ice sheet indentation, where the crushed ice flows up and down.

In 1984-85, 1989 and 1990, medium-scale indentation tests were conducted adjacent to Byam Martin Island and at Hobson's Choice Ice Island by pushing spherical and flat indentors into the walls of long trenches (50-65 m long, 2.5-3 m deep, and 3-3.5 m wide) at constant speeds ranging from 0.3 to 100 mm s^{-1} (Frederking et al. 1990, Masterson et al. 1993, 1999, Gagnon 1998). Besides measuring the total force and the displacement of the indentor, the researchers measured local pressure by installing pressure transducers in the faces of the spherical and flat indentors. Time-history plots of total force and displacement show typical saw-tooth and step patterns, respectively, indicating intermittent crushing with the advance of the indentor into the ice. Plots of pressures at different points on the indentor show a non-uniform distribution of very high and low pressures, indicating non-simultaneous ice crushing. They measured pressure as high as 35 MPa over small areas of contact. Plots of effective pressure vs. contact area show decreasing pressure with increasing contact area. They observed large-scale and small-scale flaking failure of ice. At low indentation rates, creep and microfracture occurred to some depth in the ice. At high rates of indentation, they observed a relatively thin layer of crushed and damaged ice, along with small areas of undamaged ice in the central part of the contact area (Frederking et al. 1990, Gagnon 1998).

During the winter of 1984–85, Masterson et al. (1999) conducted medium-scale indentation tests in three trenches excavated in a thick multi-year ice floe located adjacent to Byam Martin Island. They conducted 24 tests by pushing spherical or flat indentors into the walls of three trenches at various speeds ranging from 0.1 to 100 mm s^{-1}. They observed that the ice behavior was characteristic of plastic flow and ductile failure at indentation speeds below 3.16 mm s^{-1}, and brittle failure above this speed. During tests conducted at the transition speed of 3.16 mm s^{-1}, they measured the highest pressure and observed mixed ice behavior of ductile and brittle failures. Further, they report that the indentation speed had a first order effect on the ice pressures measured during the tests. They also report that significantly different loads and pressures were measured, depending on the mode of ice failure—ductile, brittle, or a combination at the transition speed. They found the effective pressure to be directly related to nominal contact area. The pressure was highest at the center and decreased with increasing radial distance. Their results from tests with flat and spherical indentors indicate that the effective pressure may strongly depend on the degree of confinement offered by the indentor shape. On the basis of their results, they recommend that the effects of indentation speed be considered for estimation of ice forces on a structure.

4. PRESSURE-AREA CURVE

The pressures developed during indentation into an ice wall are expected to be different from those during indentation into the edges of a floating ice sheet because of differences in geometry and confinement. For a spherical indentor moving into an ice wall, it is possible that

the ratio of actual to nominal contact area decreases with an increase in nominal contact area, thereby leading to a decrease in effective pressure (Masterson and Frederking 1993). This decreasing trend in the pressure-vs.-area plot for wall indentation should not be confused with the issue of scaling results from one scale to another. If the effective pressure decreases with an increase in the size of the contact area, as proposed by Sanderson (1988), the effective pressure measured during small-scale indentation tests should be much higher than the pressures measured on full-scale structures. However, a comparison of the data from full-scale measurements and small-scale indentation tests shows that the effective pressures at these two scales are close to each other when the indentation speed is high enough to cause brittle crushing in both cases. The effective pressure depends on the rate of indentation, which affects the mode of ice crushing. The issue of scaling requires similarity of geometry, kinematics, and dynamics of the processes taking place at different scales. Agreement between small-scale and full-scale data indicates that there is no size effect. Instead, there is a speed effect, leading to ductile and brittle crushing of ice at high and low effective pressure, respectively.

5. SUMMARY

The results of small-scale and medium-scale indentation tests indicate that ductile and brittle modes of ice crushing depend on the rate of indentation. A transition in the mode of ice behavior was found to be at an indentation speed between 0.3 and 3 mm s^{-1} for edge indentation of a sheet of sea ice. A transition speed of 3.16 mm s^{-1} has been reported for spherical indentors moving into an ice wall.. Each cycle of an intermittent crushing event during ice interaction with a compliant structure is a combination of ductile and brittle crushing, depending on the actual indentation rate into an ice sheet. Thus there are two transition speeds in the case of during ice interaction with a compliant structure: (a) from continuous ductile crushing to intermittent crushing, and (b) from intermittent crushing to continuous brittle crushing.

Many investigators empirically found effects of aspect ratio on the effective pressure during small-scale indentation tests for brittle crushing. Experimental verification of the actual contact area near the edge of an indentor reveal that the line-like contact is in the middle of an ice sheet across the width of an indentor. The aspect ratio effect has been derived assuming non-simultaneous crushing failure of an ice sheet. To deduce global effective pressure from measurements of local pressure over a limited area, the consideration of non-simultaneous ice crushing gives a ratio of local to global pressures in the range of 1 to 3 for 1-m-thick ice sheet crushing against a 2.27-m-wide Medof panel installed on the 59-m-wide face of the Molikpaq structure.

The results of medium-scale indentation into an ice wall have similarities to edge indentation of an ice sheet in terms of the existence of line-like contacts and a ductile-to-brittle transition speed. However, the results from these tests should not be compared to those from edge indentation of an ice sheet because of different geometry and confinement for the ice–structure interaction. Therefore, the results of decreasing effective pressure with an increasing contact area may be a result of the decreasing area of the actual contact area with indentation distance because of brittle fracture, not ascribable to size effect.

6. REFERENCES

Afanasyev, V.P., Dolgopolov, Iu.V., and Shvashteyn, Z.I. (1972) Ice pressure on separate supporting structures in the sea. Draft Translation 346, U. S. Army Cold Regions Research and Engineering Laboratory, Hanover, New Hampshire.

Ashby, M.F., Palmer, A.C., Trouless, M., Goodman, D.J., Howard, M.W., Hallam, S.D., Murrell, S.A.F., Jones, N., Sanderson, J.O., and Ponter, A.R.S. (1986) Non-simultaneous failure and ice loads on structures. In *Proceedings, Offshore Technology Conference, Houston, Texas*, p. 399–404.

Baker, W.E., Westine, P.S. and Dodge, F.T. (1973) *Similarity Methods in Engineering Dynamics.* Spartan Books, Hayden Book Company, Inc., Rochelle Park, New Jersey.

Benoit et al. (1984) Medium-scale iceberg impact tests. Video tape shown at the Arctic Offshore Technology Conference, Calgary, Alberta, Canada

Dunwoody, A.B. (1991) Non-simultaneous ice failure. A report to Amoco Production Company, Tulsa, Oklahoma.

Frederking, R.M.W., Jordaan, I.J., and McCallum, J.S. (1990) Field tests of ice indentation of medium scale, Hobson's Choice Ice Island, 1989. In *Proceedings, 10th IAHR Symposium on Ice, Espoo, Finland*, vol. 2, p. 931–944.

Gagnon, R.E. (1998) Analysis of visual data from medium scale indentation experiments at Hobson's Choice Ice Island. *Cold Regions Science and Technology*, 28: 45–58.

Hardy, M.D., Jefferies, M.G., Rogers, B.T., and Wright, B.D. (1998) DynaMAC: Molikpaq ice loading experience. PERD/CHC Report 14-62, Klohn-Crippen, Calgary, Alberta, Canada.

Hill, R. (1950) *Theory of Plasticity.* University Press, Oxford.

Joensuu, A., and Riska, K. (1989) Contact between ice and structure (in Finnish). Laboratory of Naval Architecture and Marine Engineering, Helsinki University of Technology, Espoo, Finland, Report M-88.

Kry, P.R. (1978) A statistical prediction of effective ice crushing stress on wide structure. In *Proceedings, 4th IAHR Symposium on Ice Problems, Lulea, Sweden*, p. 33–47.

Masterson, D.M., and Frederking, R.M.W. (1993) Local contact pressures in ship/ice and structure/ice interaction. *Cold Regions Science and Technology*, 3(4): 305–321.

Masterson, D.M., Frederking, R.M.W., Jordaan, I.J., and Spencer, P.A. (1993) Description of multi-year ice indentation tests at Hobson's Choice Ice Island - 1990. In *Proceedings, 12th International Conference on Offshore Mechanics and Arctic Engineering (OMAE), Glasgow, Scotland, UK*, vol. IV, p. 145–155.

Masterson, D.M., Spencer, P.A., Nevel, D.E., and Nordgren, R.P. (1999) Velocity effects from multi-year ice tests. Proceedings, 18th International Offshore Mechanics and Arctic Engineering Conference, St. John's, Newfoundland, Canada, ASME Publication, in press.

Neth, V. (1989) Rubble formation along the Molikpaq at Tarsuit P-45 during 1984/85. A report submitted by Gulf Canada Resources Ltd. to National Research Council of Canada, Vol. 1, CRREL Bib. # 46-3592.

Ponter, A.R.S., Palmer, A.C., Goodman, D.J., Ashby, M.F., Evans, A.G., and Hutchinson, J.W. (1983) The force exerted by a moving ice sheet on an offshore structure. *Cold Regions Science and Technology*, 8: 109–118.

Sanderson, T.J.O. (1988) *Ice Mechanics: Risks to Offshore Structures*. Graham and Troutman, London.

Sodhi, D.S. (1991) Ice–structure interaction during indentation tests. In *Ice–Structure Interaction: Proceedings of IUTAM-IAHR Symposium*, edited by S. Jones et al. Springer-Verlag, Berlin, p. 619–640.

Sodhi, D.S. (1992) Ice–structure interaction with segmented indentors. In *Proceedings, 11th IAHR Symposium on Ice 1992, Banff, Alberta, Canada*, vol. 2, p. 909–929.

Sodhi, D.S. (1995) An ice–structure interaction model. In *Mechanics of Geomaterial Interfaces*, edited by A.P.S. Selvadurai and M.J. Boulon. Elsevier Science B.V., Amsterdam, p 57–75.

Sodhi, D.S. (1998) Non-simultaneous crushing during edge indentation of freshwater ice sheets. *Cold Regions Science and Technology*, 27: 179–195.

Sodhi, D.S., Takeuchi, T., Nakazawa, N., Akagawa, S., and Saeki, S. (1998) Medium-scale indentation tests on sea ice at various speeds. *Cold Regions Science and Technology*.

Spencer, P.A., and Masterson, D.M. (1993) A geometrical model for pressure aspect-ratio effects in ice–structure interaction. In *Proceedings, 12th International Conference on Offshore Mechanics and Arctic Engineering (OMAE), Glasgow, Scotland, UK*, vol. IV, p. 113–117.

Wright, B., Pikington, G.R., Woolner, K.S., and Wright, W.H. (1986) Winter ice interactions with an arctic offshore structure. In *Proceedings, 8th IAHR Symposium on Ice, Iowa City, Iowa*, vol. II, p. 49–73.

Wright, B.D. and Timco, G.W. (1994) A review of ice forces and failure modes on the Molikpaq. In *Proceedings, 12th IAHR Symposium on Ice, Trondheim, Norway,* vol. 2, p. 816–825.

7. ACKNOWLEDGMENT

The author is grateful to Exxon Production Research Company for funding part of this work.